COMMUNICATIONS IN APPLIED NUMERICAL METHODS, Vol. 5, 7–14 (1989)

CALCULATION OF INTERIOR VALUES BY THE BOUNDARY ELEMENT METHOD

KEITH D. PAULSEN
Department of Electrical and Computer Engineering, University of Arizona, Tucson, AZ 85721, U.S.A.

AND

DANIEL R. LYNCH
Thayer School of Engineering, Dartmouth College, Hanover, NH 03755, U.S.A.

SUMMARY

The boundary element method (BEM) provides a straightfoward mechanism for calculating interior values once the appropriate boundary values have been determined. However, the interior solution near the boundary can exhibit unusual behaviour resulting in large numerical inaccuracies. This 'boundary layer' effect has been noted but is largely unexplored in the BEM literature. In this paper the numerical inaccuracies are shown to stem from the inability of the quadrature to account for the Green's function near-singularity. A simple scheme, which adds little extra computational effort, is used to remove the numerical inaccuracies at interior points close to the boundary by increasing the quadrature in the nearby boundary elements.

INTRODUCTION

The boundary element method (BEM) is rapidly joining the finite element method (FEM) as an established numerical technique for solving complex engineering and physics problems. The increasing popularity of the BEM is shown by its expanding use in a variety of different disciplines (see e.g. References 1–4). The primary emphasis in the BEM literature has been on the set of algebraic equations involving the knowns and unknowns on the boundaries, with significantly less attention paid to the calculation of interior values. This emphasis is appropriate; among other things the computation is largely devoted to the formulation and inversion of the boundary value matrix. The mechanism for calculating interior values appears straightfoward, and less analysis has been devoted to its accuracy. However, the interior solution can exhibit unusual behaviour, resulting in large numerical inaccuracies near the boundary.

The nature of the interior solution has been described in Reference 4. A 'boundary layer' effect has been noted which results in a degradation in the accuracy of the interior solution if the desired calculation point lies too close to the boundary. This effect has been associated with the apparent ambiguity in the recipes for computing boundary values and their immediate interior neighbours. For example, in the standard BEM representation of the Helmholtz equation (equation (4) below), the coefficient α changes abruptly from $\frac{1}{2}$ on a smooth boundary to unity at an adjacent interior point.

While the observed thickness of the boundary is problem dependent, a general rule of thumb developed in Reference 4 is that if values at interior points closer to the boundary than one

0748–8025/89/010007–08$05.00

Received 15 March 1988
Revised 21 June 1988

element's length are computed, then numerical inaccuracies can occur. The remedy prescribed is either to avoid calculation in the boundary layer (impossible in an operational setting) or to increase the boundary discretization in order to reduce the thickness of the layer.

This heuristic remedy has two problems. First, it is not linked causally to any theoretical explanation of the error. The integral statements themselves and the apparent jump in the value of α are completely sound products of classical analysis—suggesting that the numerical implementation of the boundary integrals is at fault. Second, it scales unfavourably. To cut the boundary layer in half requires a doubling of the number of nodes, with attendant increases by a factor of 2^2 in matrix storage and 2^3 (for direct methods) in matrix inversion run-time alone. Essentially, one is over-resolving the problem simply to be able to sample a smooth solution near the boundary, thus artificially constraining the size of practical problems which can be considered.

In our experience with the BEM, we have observed this boundary layer phenomenon as well. Our purpose in this paper is (1) to illustrate and quantify the serious errors that can occur in the boundary layer, (2) to provide a theoretically sound explanation for the existence of these errors, and (3) to show a simple and cost-effective scheme which we have implemented for removing the errors in our BEM codes.

METHODS

Our involvement with the BEM has been in the context of solving Maxwell's equations for simulating the hyperthermic treatment of cancer. Both two and three dimensional formulations have been studied in which the BEM has been used either alone or in hybrid fashion with the FEM.[5-8] When coupled with the FEM, the BEM equations provide a formal solution to the problem of a detached source delivering energy to a highly heterogeneous body embedded in an unbounded domain. We first encountered the boundary layer effect in testing our BEM codes against known analytic solutions.

The BEM formulation which we have developed is based on the integral equation

$$-\oint_s j\omega\mu(\hat{\mathbf{n}}\times\mathbf{H})G_i\,da = \alpha_i E_i + \oint_s (\hat{\mathbf{n}}\times\mathbf{E})\times\nabla G_i\,da + \oint_s (\hat{\mathbf{n}}\cdot\mathbf{E})\nabla G_i\,da \tag{1}$$

where

$\mathbf{E}$ = complex amplitude of the electric field
$\mathbf{H}$ = complex amplitude of the magnetic field
$j = \sqrt{-1}$
$\hat{\mathbf{n}}$ = outward-pointing unit normal vector to the surface
$\varepsilon^* = \epsilon + j\sigma/\omega$ is the complex permittivity
ϵ = permittivity
σ = electrical conductivity
μ = magnetic permeability
ω = angular frequency

In equation (1), G_i is the unbounded space Green's function satisfying the Helmholtz equation with a singularity at $\mathbf{x} = \mathbf{x}_i$:

$$\nabla^2 G_i + \omega^2\mu\varepsilon^* G_i = -\delta(\mathbf{x} - \mathbf{x}_i) \tag{2}$$

and α_i is the volume or domain integral of the delta function in equation (2):

$$\alpha_i = \int_V \delta(\mathbf{x} - \mathbf{x}_i)\, dV \tag{3}$$

Note that when $\mathbf{x}_i$ is in the interior α_i is unity, while for $\mathbf{x}_i$ on the boundary α_i is less than unity ($\frac{1}{2}$ for smooth boundaries).

By enforcing N (where N is the number of boundary nodes) versions of equation (1) using the set of Green's functions such that G_i is singular at the ith node, a matrix of algebraic equations can be generated. This resulting matrix equation provides a mechanism for calculating $\mathbf{E}$ on a closed boundary, given that $\hat{\mathbf{n}} \times \mathbf{H}$ is known on that boundary, and vice versa. Once both $\mathbf{n} \times \mathbf{H}$ and $\mathbf{E}$ are known over the boundary, then $\mathbf{E}$ can be calculated everywhere inside the domain contained by this boundary via equation (1) with α_i equal to unity.

In two dimensions, equation (1) reduces to

$$\alpha_i E_{z,i} = \oint_s (\hat{\mathbf{n}} \cdot \nabla E_z) G_i \, da - \oint_s E_z (\hat{\mathbf{n}} \cdot \nabla G_i) \, da \tag{4}$$

when $\mathbf{E}$ is perpendicular to the analysis plane (denoted by the subscript z). Equation (4) is readily recognized as a boundary integral of the scalar Helmholtz equation. Because it is more familiar and simpler than equation (1), equation (4) is used below. We note in passing that a dual formulation, mathematically equivalent to equations (1) and (4), is available for the magnetic field.[5]

ANALYSIS

Equation (4) suffices as a recipe for boundary as well as interior values of $\mathbf{E}$, provided α_i is properly interpreted according to equation (3). The apparent contradiction at or near the boundary in the value of α_i is resolved by noting that the right hand side integrals in equation (4) imply different operations, as illustrated in Figure 1. When $\mathbf{x}_i$ is on the boundary, the integrand is singular and equation (4) calls for the Cauchy principal value (Figure 1(a)). This in turn is commonly evaluated analytically, thus introducing no additional numerical error in the integration. However, when $\mathbf{x}_i$ is in the interior the integrand is smooth, bounded and continuous, and the integral is well-defined and obtainable by quadrature (Figure 1(b)). However, when $\mathbf{x}_i$ is close to the boundary, the integrand is near-singular and special care in the quadrature is needed to avoid introducing large numerical errors. This is the source of the boundary layer problem—the integral formulations are perfectly well-posed, but their evaluation by quadrature can be grossly imperfect if $\mathbf{x}_i$ is too close to the boundary.

The conventional prescription of reducing the boundary element size evidently works by indirectly introducing more quadrature points into the near-singular area, as shown in Figure 1(c). It is apparent that one may expect relatively slow convergence from this approach, and in the light of the above scaling arguments, at significant computational expense. Instead, we advocate a more direct solution—simply increase the level of quadrature in those elements which are less than one boundary layer away from the interior evaluation point (Figure 1(d)). This simple adaptation, which can be realized in any BEM code, places no additional demands on the basic boundary discretization, and requires only a small additional amount of computing during the post-processing step when the desired interior values are calculated.

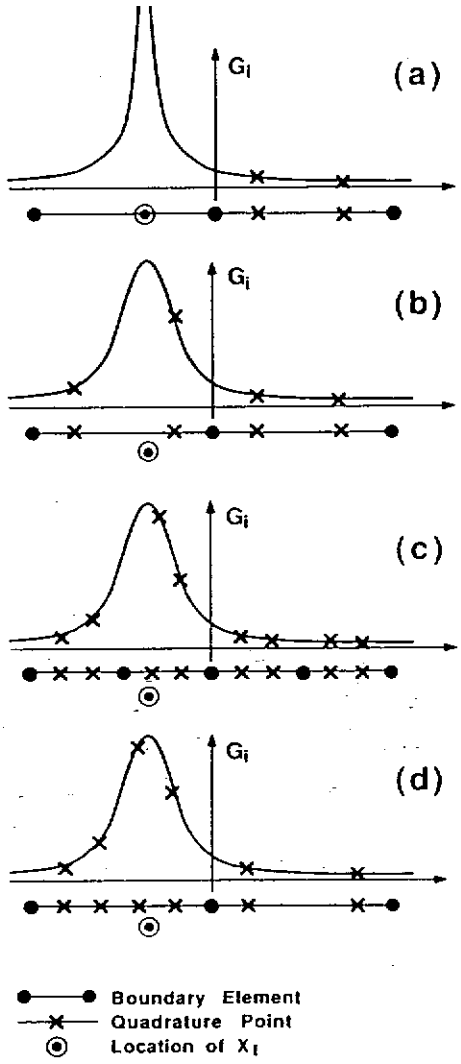

Figure 1. Illustration of boundary integration of singular G_i. (a) x_i on the boundary; integration over singularity achieved analytically. (b) x_i near the boundary; quadrature too crude. (c) indirect improvement in quadrature by halving the boundary element. (d) direct improvement in quadrature by increasing the number of Gauss points

RESULTS

Equation (4) has been solved for a simple concentric cylinder geometry where a uniform value of E_z was imposed on the outer boundary, and 24 linear boundary elements were used to discretize each surface. The two cylinders were composed of different dielectrics (inner cylinder: $\varepsilon = 40\varepsilon_0$, $\sigma = 0{\cdot}35\ \Omega^{-1}\,m^{-1}$; outer cylinder: $\varepsilon = 85\varepsilon_0$, $\sigma = 0{\cdot}802\ \Omega^{-1}\,m^{-1}$), their radii were 12 and 25 cm, and the excitation frequency was 70 MHz. The numerical solution for interior points near the outer cylinder was compared to the analytic solution, which can be found elsewhere.[8] Results from these computations appear in Figures 2–5.

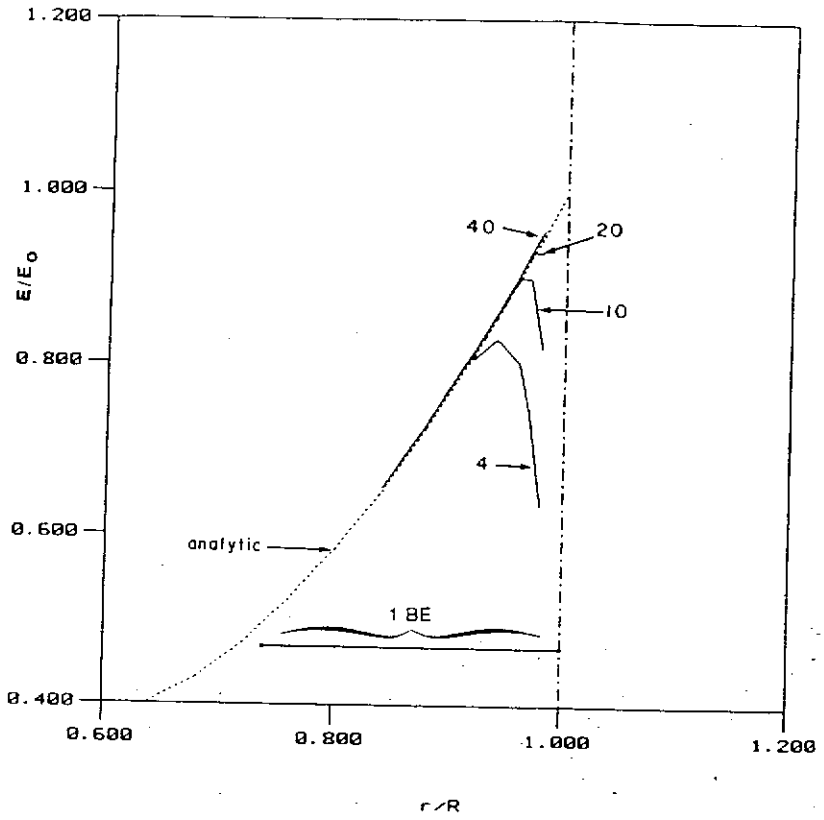

Figure 2. Interior BEM solution of $|E_z|$ within the 'boundary layer'. The boundary is approached along a radius which intersects the centre of a boundary element ($\theta = 7.5^\circ$ in Figure 3). The selective increase in the Gauss points used in a boundary element (BE) within 1 BE of x_i is indicated. All other integrations involved four quadrature points

Figure 2 shows the numerical value of $|E_z|$ near the boundary versus radius for increasing numbers of Gauss points. The interior point closest to the boundary is at $r = 0{\cdot}98\ R$, while the length of the boundary elements is $0{\cdot}26\ R$ (displayed in Figure 2). Figure 3 shows the circumferential variation of the computed $|E_z|$ at a fixed radius, $r = 0{\cdot}98\ R$, for increasing numbers of quadrature points. As these figures illustrate, the boundary layer effect can indeed be severe, but can be remedied for a given boundary discretization by selectively increasing the quadrature.

Figures 4 and 5 show that judicious selection of the Gauss points can significantly reduce the number of stations needed (in nearby boundary elements) for accurate evaluation of interior values close to the boundary. The difference between these figures and Figures 2 and 3 is that here the non-linear co-ordinate transformation reported by Telles[9] has been implemented. The transformation 'bunches up' the Gauss points around a specified location along the integration path. By choosing this position as the point along a given nearby boundary element where the Green's function is most nearly singular, Gauss points are concentrated where they are needed most—a desirable feature, as illustrated in Figure 1(d)—while the accuracy of the near-singular integrals is maintained with lower-order quadrature.

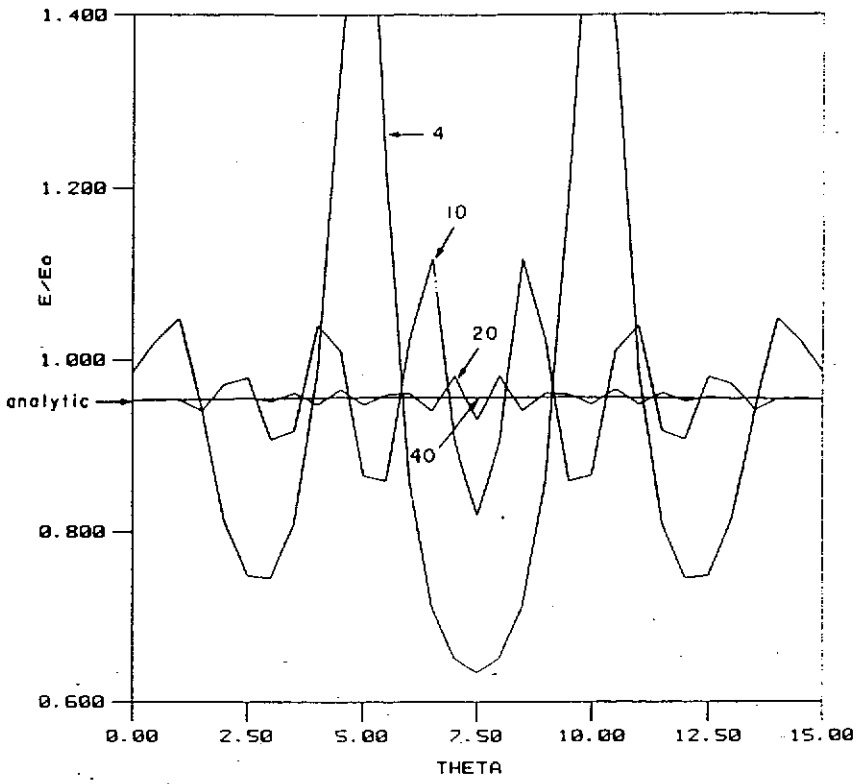

Figure 3. $|E_z|$ versus arc length θ along a boundary element at a fixed radius $r = 0{\cdot}98\ R$. The selective increase in the Gauss points is indicated

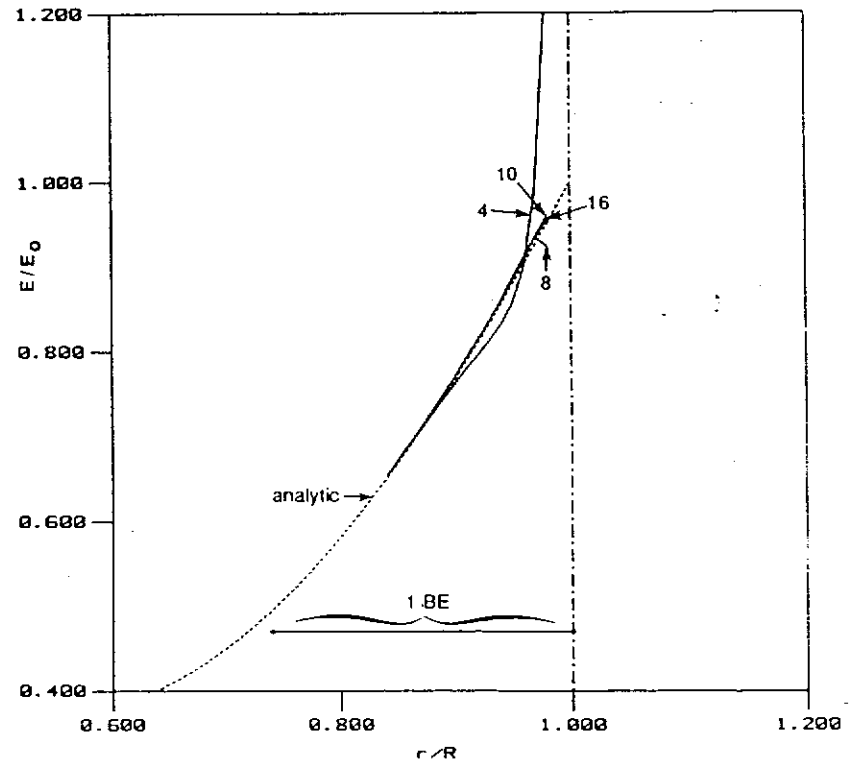

Figure 4. As Figure 2, except that a co-ordinate transformation has been used to concentrate the Gauss points in nearby boundary elements around the location where the Green's function is most nearly singular

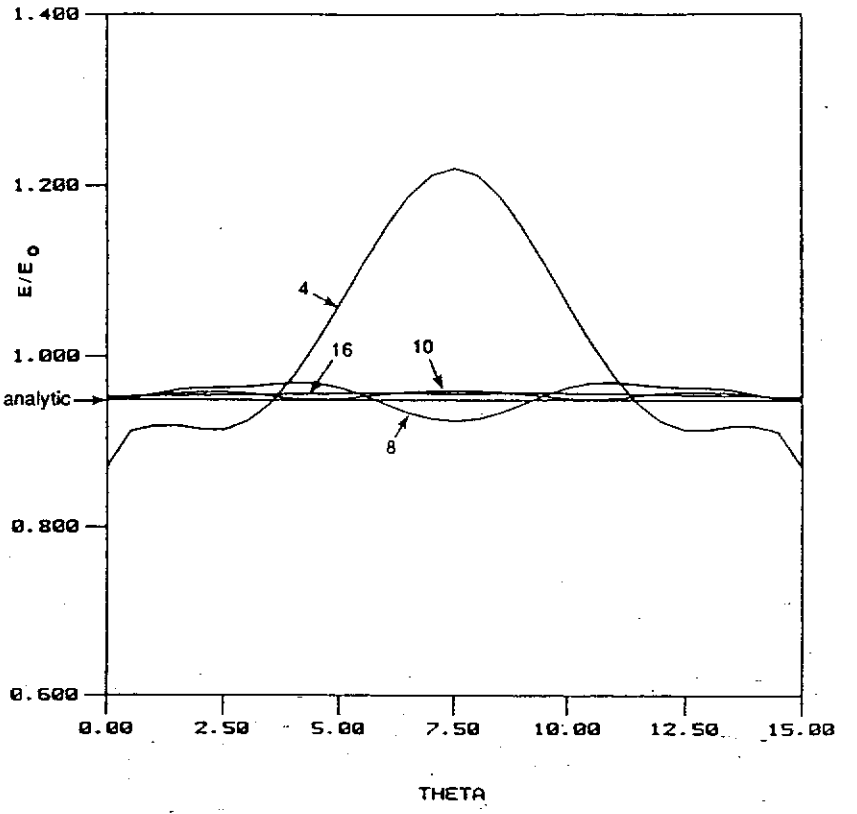

Figure 5. As Figure 3 except that a co-ordinate transformation has been used to concentrate the Gauss points in nearby boundary elements around the location where the Green's function is most nearly singular

CONCLUSION

Calculation of interior values with the BEM can be seriously compromised if the point of interest is close to the boundary. The numerical inaccuracies stem from the inability of simple quadrature to account for the near-singular behaviour of the Green's function in elements which are 'too close' to the interior point. The problem can be overcome, at only a small additional cost, by increasing the level of quadrature in these elements and so avoiding more computationally expensive remedies such as increasing the boundary discretization. By defining the boundary layer conservatively, for example as the length of the largest boundary element, it is a simple matter to increase the quadrature as needed during the element-by-element assembly of the boundary integrals for any given interior point. Co-ordinate transformations, which 'bunch' the Gauss points around the most near-singular points of nearby boundary element integrations, reduce the order of any extra quadrature. Other more sophisticated or problem-dependent measures of the boundary layer thickness are easily accommodated.

ACKNOWLEDGEMENT

This work was supported by the National Science Foundation, Grant No. CEE-8352226, and by the National Cancer Institute, Grant Nos. R01-37245-04 and R29-CA45357-02.

REFERENCES

1. C. A. Brebbia (Ed.), *Topics in Boundary Element Research. Volume 1: Basic Principles and Applications*, Springer-Verlag, Berlin, 1984.
2. C. A. Brebbia. (Ed.) *Topics in Boundary Element Research Volume 2: Time-dependent and Vibration Problems*, Springer-Verlag, Berlin, 1985.
3. T. A. Cruse, 'Recent advances in boundary element analysis methods', *Computer Methods Appl. Mech. Eng.*, **62**, 227–244 (1987).
4. J. A. Liggett and P. L-F. Liu, *The Boundary Integral Equation Method for Porous Media Flow*, George Allen and Unwin, London, 1983.
5. D. R. Lynch, K. D. Paulsen and J. W. Strohbehn, 'Hybrid element method for unbounded electromagnetic problems in hyperthermia', *Int. j. numer. methods eng.*, **23**, 1915–1937 (1986).
6. K. D. Paulsen, J. W. Strohbehn and D. R. Lynch, 'Theoretical electric field distributions produced by three types of regional hyperthermia devices in a three-dimensional homogeneous model of a man', *IEEE Trans. Biomed. Eng.*, **BME-35**, 36–45 (1988).
7. K. D. Paulsen, D. R. Lynch and J. W. Strohbehn, 'Three-dimensional finite, boundary, and hybrid element solutions of the Maxwell equations for lossy dielectric media', *IEEE Trans. Microw. Theory Tech.*, **MTT-36**, 682–693 (1988).
8. D. R. Lynch, K. D. Paulsen, and J. W. Strohbehn, 'Finite element solution of Maxwell's equations for hyperthermia treatment planning', *J. Comput. Phys.*, **58**, 246–269 (1985).
9. J. C. F. Telles, 'A self-adaptive co-ordinate transformation for efficient numerical evaluation of general boundary element integrals', *Int. j. numer. methods eng.*, **24**, 959–973 (1987).